frontiers | Frontiers in Sustainable Food Systems

TYPE Original Research
PUBLISHED 28 April 2025
DOI 10.3389/fsufs.2025.1590775

OPEN ACCESS

EDITED BY
Guihun Jiang,
Jilin Medical University, China

REVIEWED BY
Beatriz Mello,
Federal University of São Carlos, Brazil
José Armando Ulloa,
Autonomous University of Nayarit, Mexico

*CORRESPONDENCE
Zhengyu Hu
✉ 0000007948@ybu.edu.cn
Gao Li
✉ gli@ybu.edu.cn

RECEIVED 10 March 2025
ACCEPTED 04 April 2025
PUBLISHED 28 April 2025

CITATION
Duan Y, Jiang Y, Gu J, Sun C, Sun B, Xu Y, Jin L, Jin M, Sun J, Zhou W, Hu Z and Li G (2025) Ultrasonic-assisted extraction of polysaccharides from *Albizia julibrissin* Durazz. leaf and pod: process optimization, physicochemical properties and anticomplementary activity. *Front. Sustain. Food Syst.* 9:1590775. doi: 10.3389/fsufs.2025.1590775

Ultrasonic-assisted extraction of polysaccharides from *Albizia julibrissin* Durazz. leaf and pod: process optimization, physicochemical properties and anticomplementary activity

Yuanqi Duan[1], Yuxin Jiang[1], Jiayu Gu[1], Chenxi Sun[1], Boshi Sun[1], Yue Xu[1], Long Jin[1], Mei Jin[1,2], Jinfeng Sun[1], Wei Zhou[1], Zhengyu Hu[1]* and Gao Li[1]*

[1]Key Laboratory of Natural Medicines of the Changbai Mountain, Ministry of Education, College of Pharmacy, Yanbian University, Yanji, China, [2]Department of Pharmacy, Yanbian University Hospital, Yanji, China

This study employed ultrasound-assisted extraction to obtain polysaccharides from *Albizia julibrissin* Durazz. leaf and pod agricultural by-products, with subsequent process optimization. A comparative analysis was then conducted on the physicochemical properties and anticomplementary activity of the isolated polysaccharides derived from two parts. The investigation identified different extraction conditions for leaf and pod, leaf demonstrated maximum polysaccharide yield (1.07 ± 0.20%) at 70°C, 40 mL/g, 50 min and 249 W, contrasting with pod which achieved 8.32 ± 0.27% yield at 70°C, 28 mL/g, 40 min and 201 W. Besides, physicochemical characterization demonstrated distinct molecular weights between leaf (AJLP) and pod (AJPP) polysaccharides (62.55–232.30 kDa) despite shared functional groups. Both polysaccharides contained mannose, rhamnose, glucuronic acid, galacturonic acid, glucose, galactose, xylose, and arabinose in varying ratios, while displaying divergent microstructures and excellent thermal stability. *In vitro*, leaf (AJLP) and pod (AJPP) polysaccharides exhibited potent anticomplementary activity in alternative and classical pathways, respectively. This study established a foundation for developing and utilizing polysaccharide resources from *A. julibrissin* agro-byproducts, while providing a theoretical basis for their application in complement system overactivation.

KEYWORDS

***Albizia julibrissin* Durazz., different parts, agroindustrial subproducts, polysaccharides, characterization**

1 Introduction

Albizia julibrissin Durazz., belonging to the Fabaceae family, is a deciduous tree capable of reaching a height of 16 m (Nehid, 2011). In the context of traditional Chinese medicine, *A. julibrissin's* flower and bark are routinely used for medicinal applications (Lau et al., 2007; Han et al., 2011). Previous research endeavors primarily centered on the flower or bark constituents, such as triterpenoids, flavonoids, lignans, phenols, alkaloid. As these constituents demonstrated diverse pharmacological activities, including anti-inflammatory, antioxidant, antitumor effects, immune regulation, and antidepressant

properties (Huang et al., 2023; Lu et al., 2023; He et al., 2020). With the increasing demand of *A. julibrissin* bark and flower in recent years, their production is difficult to meet the market demand. Therefore, seeking the high efficiency of the replaceable medicinal parts and their bioactive constituents is the key to promote the comprehensive development and utilization of *A. julibrissin* at present. Meanwhile, as agro-byproducts, the leaf and pod have largely remained uninvestigated in terms of their chemical constituents and biological properties to date. Since these parts are not used medicinally, they are often discarded, leading to a certain degree of environmental pollution and economic losses. However, polysaccharides, as one of the most promising active ingredients with significant development potential in agro-byproducts, have rarely been reported.

Polysaccharides are a kind of natural macromolecular polymers that widely exist in various agro-byproducts, composed of more than 10 monosaccharides linked by glycosidic bonds, with molecular weights varying from thousands to millions (Xiu et al., 2023). These large molecules have crucial functions in a wide range of biological processes, encompassing intercellular recognition and communication, defense, biosynthetic reactions, signaling, cell proliferation, and immunity (Wang W. et al., 2023). Numerous research efforts have shown that polysaccharides offer diverse health advantages, coupled with good hydrophilicity, safe profiles, and biodegradability, leading to their broad utilization in the food, pharmaceutical, and industrial sectors (Zhang Y. et al., 2023). Recently, various polysaccharide constituents from agro-byproducts, including *Panax ginseng* C. A. Meyer stems (Xu et al., 2024), mulberry twigs (Liu et al., 2023), and *Pleurotus ostreatus* stipes (Jean et al., 2025), have been reported and demonstrated to possess hypoglycemic, antioxidant, and wound-healing properties.

Complement is a crucial element of the innate immune system during homeostasis functions as well as during host defense (Andrew et al., 2024). However, when the activation of the complement system is out of balance, it leads to an excessive inflammatory response, which can cause the onset and progression of a variety of diseases, including systemic lupus erythematosus, acute respiratory distress syndrome, Alzheimer's disease (Jacqui et al., 2024; Wang X. et al., 2023; Ruth and Howard, 2022), seriously affecting human health. Currently, although there are several drugs used to treat diseases related to complement overactivation, these drugs often lack selectivity, are costly, and may cause adverse reactions. This highlights the need for further research into safer, more affordable, and effective alternatives, such as polysaccharides, which may offer new therapeutic possibilities in this area. Meanwhile, polysaccharides from agricultural by-products with potential applications in complement system overactivation related diseases remain scarcely reported.

Therefore, for the first time, this study innovatively utilized ultrasound-assisted extraction to obtain polysaccharides from the agro-byproducts of *A. julibrissin* leaf and pod, followed by optimization of the extraction process. And then, leaf (AJLP) and pod (AJPP) polysaccharides were isolated by column chromatography, and a comparative analysis was conducted on the physicochemical properties and anticomplementary activity. This research offers a theoretical foundation for the comprehensive utilization of *A. julibrissin*, a traditional Chinese medicine, and can yield economic benefits. In addition, these findings significantly enriched our understanding of the anticomplementary activity of polysaccharides derived from agricultural by-products, while providing essential research materials for investigating complement overactivation related diseases.

2 Materials and methods

2.1 Materials and chemicals

Albizia julibrissin Durazz. leaf and pod were procured at the Bozhou Chinese herb market in Anhui, China. Shanghai Aladdin Bio-Chem Technology Co., LTD. supplied the trifluoroacetic acid (TFA). The Guangzhou Hongquan Biological Technology Company, situated in Guangzhou, China, produced the human serum. Erythrocyte extraction was performed utilizing Alsever's solution, originally sourced from male sheep and rabbits. The essential reagents, all of HPLC quality, were obtained from commercial vendors. The entire experimental process adhered strictly to the guidelines set by the National Institutes of Health for the Care and Use of Laboratory Animals. Ethical approval was also obtained from Yanbian University's Ethics Committee, with approval number YBU-2018-090401.

2.2 Optimization design for ultrasound-assisted extraction of polysaccharides

Polysaccharides from *A. julibrissin* leaf and pod were extracted utilizing an ultrasonic extractor (JM-15D-28, Skymen, China). The extraction process involved varying four parameters: extraction time (20 min to 60 min), temperature (40°C to 80°C), liquid solid ratio (10 mL/g to 50 mL/g), and ultrasonic power (100 W to 300 W). Based on the results of the single-factor test, the preliminary ranges for extraction temperature (X_1, °C), liquid-to-solid ratio (X_2, mL/g), ultrasonic time (X_3, min), and ultrasonic power (X_4, W) were determined. The extraction process conditions were optimized using RSM (Hao et al., 2023). Additionally, the yield of polysaccharide served as the response value, with each experiment replicated three times. Subsequently, the experimental data obtained from the Box–Behnken Design (BBD) were analyzed using Design Expert 13.0 software (Li et al., 2018).

2.3 Polysaccharides purification

The crude polysaccharides underwent precipitation using 80% ethanol, followed by deproteinization via the Sevag method (Yuan et al., 2024). Further purification involved loading the polysaccharides onto a DEAE-52 cellulose column (2.6 cm × 60 cm) and eluted using 0.5 mol/L NaCl solution at a flow rate of 1 mL/min, subsequently dialyzing through a membrane with a 8,000 Da cutoff.

2.4 Chemical composition and purity analysis

Chemical composition and purity analysis were conducted on the polysaccharide constituents of leaf and pod before

(crude-AJLP and crude-AJPP) and after (AJLP and AJPP) purification. The measurement of the total polysaccharide content was performed using the phenol-sulfuric acid approach, with absorbance precisely quantified at 490 nm. For quantifying polyphenol and flavonoids content, the Folin–Ciocalteu method and aluminum trichloride assay were employed, where the absorbance was precisely measured at 530 nm. Furthermore, the Bradford method employing Coomassie blue G250 dye was utilized to evaluate the protein content, with absorbance meticulously measured at a wavelength of 595 nm. Meanwhile, the content of uronic acid was determined with precision using the meta-hydroxydiphenyl method, with absorbance accurately quantified at 520 nm (Niu et al., 2017; Duan et al., 2024; Kanlayavattanakul et al., 2019).

2.5 Fourier transform infrared analysis

This test involved mixing each polysaccharide fraction with an appropriate amount of KBr, then compressing the mixture into tablets, and using fourier transform infrared spectroscopy (FTIR, Thermo Science Nicolet iS20, Thermo Fisher, United States) to scan the wavenumber spectrum from 4,000 to 400 cm^{-1}.

2.6 Molecular weight distribution determination

The molecular weight (Mw) of the polysaccharides was assessed using high-performance gel permeation chromatography (GPC) equipped with a RID-20A detector (Shimadzu, Japan). The samples were diluted to a concentration of 2 mg/mL for analysis. Chromatographic Conditions: A Shodex sugar KS-804 column (7 μm, 8.0 mm × 300 mm) was utilized, maintained at a temperature of 40°C. The mobile phase consisted of ultrapure water, pumped through the system at a flow rate of 1.0 mL/min, and the sample was injected with a volume of 20 μL. A calibration curve, established using dextran standards of known molecular weights, was employed to determine the Mw of the polysaccharides.

2.7 Monosaccharide composition analysis

The monosaccharide composition was assessed and modified employing a method previously documented in (Liu et al., 2019). A 10 mg polysaccharide sample was hydrolyzed using 2 mol/L TFA, subsequently derivatized with a solution of 0.3 mol/L NaOH, PMP-Methanol, and 0.3 mol/L HCl. To purify the derivative, the mixture was washed three times with chloroform to eliminate impurities from the aqueous layer. Subsequently, the sample was analyzed using high-performance liquid chromatography (HPLC) equipped with a 1,410 UV detector (Hitachi Primaide, Japan). The HPLC analysis was conducted on a Supersil ODS2 column (2.5 μm, 4.6 mm × 250 mm) maintained at 35°C. The elution process occurred at a flow rate of 0.8 mL/min, and the derivative was detected at a wavelength of 245 nm. The mobile phase was composed of a mixture of phosphate buffered saline (PBS) at pH 6.8 and acetonitrile in a ratio of 83:17 (v/v).

2.8 Scanning electron microscopy analysis

The microscopic morphological properties of the polysaccharides was investigated through the use of a Gemini SEM 360 (ZEISS, Oberkochen, Germany). The sample powder was placed on the specimen stage and then coated with a thin layer of gold using an ion sputtering device. This allowed for the examination of the samples at various magnifications, including 200×, 500×, 1,000 × and 2000×.

2.9 Thermal gravimetric analysis

The assessment of the thermal stability of the polysaccharide sample was conducted using a Thermal gravimetric analyzer TG 209 F1 Libra (NETZSCH-Gerätebau GmbH, Selb, Germany). In detail, a quantity of 5 mg of the sample was placed within a platinum crucible, followed by heating at a rate of 20°C/min, ranging from 30 to 800°C.

2.10 Anticomplementary activity

The polysaccharide samples' anticomplementary activity was assessed through a hemolysis test, following a previously reported method (Wang et al., 2022). For this test, a dilution of normal human serum pool (NHSP) was prepared in GVB-Ca^{2+}/Mg^{2+} buffer, using a specified ratio. The polysaccharide samples underwent subsequent dilution in the identical buffer and were preincubated with NHSP. Subsequently, sensitized sheep erythrocytes (2.0×10^9 cells/mL) or rabbit erythrocytes (5.0×10^8 cells/mL) were added. Upon completion of the reaction, the mixture underwent centrifugation, followed by precise measurement of the supernatant's optical density at a wavelength of 540 nm using a microplate reader (Infinite 200 PRO, Tecan, Switzerland). Ultimately, the CH_{50} and AP_{50} was employed to evaluate the anticomplementary activity of the tested fraction.

2.11 Statistical analysis

The outcomes of three parallel experiments ($n = 3$) were presented as mean values accompanied by their standard deviations (± SD). Significant statistical differences ($p < 0.05$) were determined through ANOVA analysis utilizing GraphPad Prism 6.0 software.

3 Results and discussion

3.1 Single factor experiments

Utilizing the conventional single factor variation approach, during each individual factor experiment, all parameters remain constant except for the one being specifically investigated. Figure 1 demonstrated the influence of four extraction parameters: extraction temperature (X_1, °C), liquid to solid ratio (X_2, mL/g), ultrasonic time (X_3, min), and ultrasonic power (X_4, W), on the yield of *A. julibrissin* polysaccharide. The findings revealed that the most favorable individual condition for maximizing leaf polysaccharide yield was ultrasonic time of 50 min, extraction temperature of 70°C, liquid to

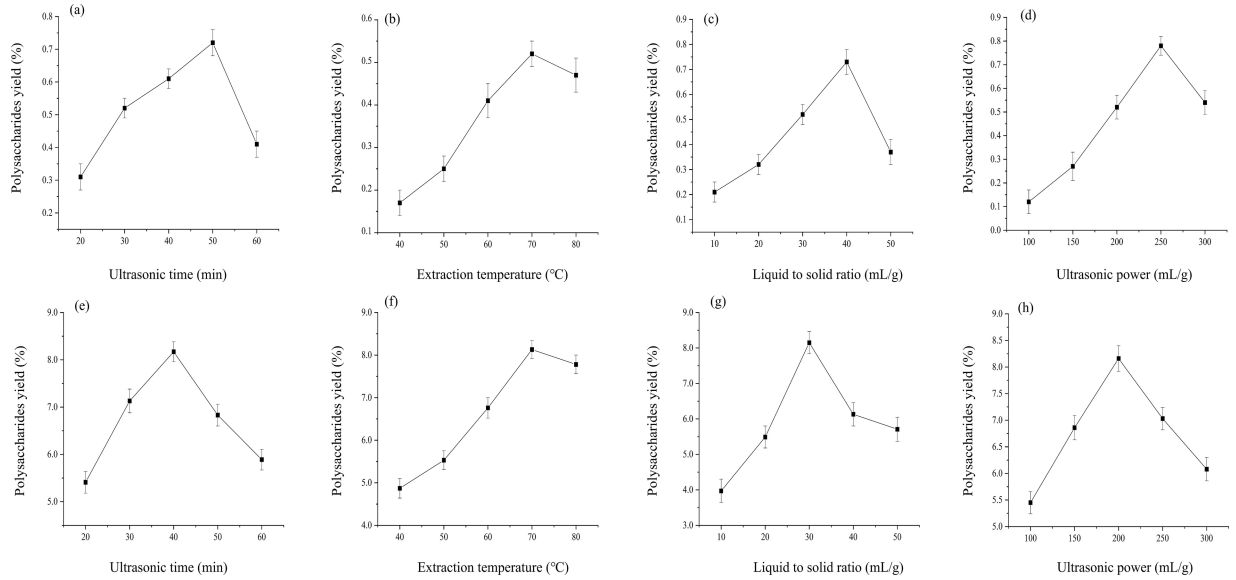

FIGURE 1
Effect of different independent factors on the extraction rates of leaf **(a–d)** and pod **(e–h)**.

solid ratio of 40 mL/g, and ultrasonic power of 250 W. Analogously, for pod polysaccharides, the optimal single parameter was 40 min, 70°C, 30 mL/g, 200 W.

The results for each of the two parts demonstrated a trend of initial increase followed by a decrease. In particular, as the temperature continued to increase, there was a noticeable decline in the extraction yield. This could potentially be attributed to excessively high temperatures disrupting the structural stability of polysaccharides, thereby promoting their oxidation and thermal degradation (Zhang et al., 2024). At higher liquid to solid ratio, the extraction yield decreased, this could be due to an increased solvent volume leading to a greater internal diffusion distance, subsequently reducing hydration and impacting mass transfer (Zheng et al., 2016). Eventually, as the ultrasound time and power increased, a declining trend was observed in the extraction yield. When prolonged ultrasound time coupled with excessive power was applied, it intensified the thermal effect and mechanical action, leading to polysaccharide molecule degradation and consequently lowering the yield (Zhang W. et al., 2023). In addition, an interesting phenomenon observed was that leaf parameters were higher in terms of ultrasonic time, liquid to solid ratio, and ultrasound power. This may be due to the fact that the cell wall structure of leaf and the binding form of polysaccharides are more complex compared to pod, requiring higher extraction time, liquid to material ratio, and ultrasound power to overcome these interactions.

3.2 Response surface for ultrasound-assisted extraction

The optimum ultrasound-assisted extraction parameters for polysaccharides from *A. julibrissin* leaf and pod were optimized using response surface methodology. The quadratic polynomial function representing the leaf (Equation 1) and pod (Equation 2) polysaccharides was expressed in order as follows:

$$Y = 1.35 + 0.0317X_1 + 0.0400X_2 + 0.0367X_3 - 0.0100X_4 + 0.0575X_1X_2 + 0.0425X_1X_3 - 0.1200X_1X_4 - 0.0900X_2X_3 + 0.0725X_2X_4 - 0.0175X_3X_4 - 0.4145X_1^2 - 0.3920X_2^2 - 0.3870X_3^2 - 0.5345X_4^2 \quad (1)$$

$$Y = 8.87 - 0.0708X_1 - 0.0033X_2 - 0.2067X_3 - 0.0008X_4 - 0.1150X_1X_2 - 0.0825X_1X_3 + 0.0500X_1X_4 + 0.1175X_2X_3 + 0.0925X_2X_4 - 0.1250X_3X_4 - 0.7508X_1^2 - 0.5021X_2^2 - 0.5321X_3^2 - 0.6458X_4^2 \quad (2)$$

The analysis of variance (ANOVA) for the quadratic polynomial model extracted from leaf and pod polysaccharides (Tables 1, 2). As displayed, the *p*-values of the model were all less than 0.0001, which meant that the model had significance. Meanwhile, the values of the regression coefficient (R^2) of leaf and pod were 0.9901 and 0.9849, respectively. The experimental data exhibited a high degree of precision and reliability, with R^2Adj above 0.90 and C.V. below 10%, indicating a strong correlation between the observed and predicted values. And, the model equation demonstrated adequate predictive capability for the extraction yield of polysaccharides, as evidenced by the negligible lack of fit (Ji et al., 2021). Consequently, these findings imply that the model was applicable for exploring the design space. Moreover, four interaction term coefficients (X_1X_2, X_1X_4, X_2X_3, and X_2X_4) significantly affected leaf polysaccharide yield, while three (X_1X_2, X_2X_3, and X_3X_4) influenced pod polysaccharide yield ($p < 0.05$). All quadratic term coefficients (X_1^2, X_2^2, X_3^2, and X_4^2) significantly impacted both yields ($p < 0.001$). The utilization of two-dimensional contour (2D) plots and three-dimensional response surface (3D) charts, depicted in Figures 2, 3, aided in elucidating the relationship between the yield of leaf and pod polysaccharides, which was influenced by four factors, and its independent and dependent variables.

TABLE 1 ANOVA for response surface quadratic model of the leaf polysaccharides yield.

Source	Sum of squares	Df	Mean square	*F*-value	*p*-value
Model	3.39	14	0.2418	99.72	< 0.0001***
X_1	0.0120	1	0.0120	4.96	0.0428*
X_2	0.0192	1	0.0192	7.92	0.0138*
X_3	0.0161	1	0.0161	6.65	0.0218*
X_4	0.0012	1	0.0012	0.4948	0.4933
X_1X_2	0.0132	1	0.0132	5.45	0.0349*
X_1X_3	0.0072	1	0.0072	2.98	0.1063
X_1X_4	0.0576	1	0.0576	23.75	0.0002***
X_2X_3	0.0324	1	0.0324	13.36	0.0026**
X_2X_4	0.0210	1	0.0210	8.67	0.0107*
X_3X_4	0.0012	1	0.0012	0.5051	0.4889
X_1^2	1.11	1	1.11	459.52	< 0.0001***
X_2^2	0.9967	1	0.9967	410.99	< 0.0001***
X_3^2	0.9715	1	0.9715	400.57	< 0.0001***
X_4^2	1.85	1	1.85	764.10	< 0.0001***
Residual	0.0340	14	0.0024		
Lack of fit	0.0120	10	0.0012	0.2196	0.9764
Pure error	0.0219	4	0.0055		
Correlation total	3.42	28			
R^2	0.9901		R^2_{Adj}	0.9801	
C.V.%	7.71		Pred R-Squared	0.9697	

*$p < 0.05$. **$p < 0.01$. ***$p < 0.001$. "X_1" denotes extraction temperature (°C); "X_2" denotes liquid to solid ratio (mL/g); "X_3" denotes ultrasonic time (min); "X_4" denotes ultrasonic power (W).

TABLE 2 ANOVA for response surface quadratic model of the pod polysaccharides yield.

Source	Sum of squares	Df	Mean square	*F*-value	*p*-value
Model	7.24	14	0.5170	65.14	<0.0001***
X_1	0.0602	1	0.0602	7.59	0.0155*
X_2	0.0001	1	0.0001	0.0168	0.8987
X_3	0.5125	1	0.5125	64.57	< 0.0001***
X_4	8.333E-06	1	8.333E-06	0.0010	0.9746
X_1X_2	0.0529	1	0.0529	6.66	0.0217*
X_1X_3	0.0272	1	0.0272	3.43	0.0852
X_1X_4	0.0100	1	0.0100	1.26	0.2806
X_2X_3	0.0552	1	0.0552	6.69	0.0195*
X_2X_4	0.0342	1	0.0342	4.31	0.0567
X_3X_4	0.0625	1	0.0625	7.87	0.0140*
X_1^2	3.66	1	3.66	460.69	< 0.0001***
X_2^2	1.64	1	1.64	206.00	< 0.0001***
X_3^2	1.84	1	1.84	231.36	< 0.0001***
X_4^2	2.71	1	2.71	340.85	< 0.0001***
Residual	0.1111	14	0.0079		
Lack of fit	0.1009	10	0.0101	3.96	0.0985
Pure error	0.0102	4	0.0025		
Correlation total	7.35	28			
R^2	0.9849		R^2_{Adj}	0.9849	
C.V.%	1.13		Pred R-Squared	0.9187	

*$p < 0.05$. **$p < 0.01$. ***$p < 0.001$. "X_1" denotes extraction temperature (°C); "X_2" denotes liquid to solid ratio (mL/g); "X_3" denotes ultrasonic time (min); "X_4" denotes ultrasonic power (W).

The ultrasound-assisted extraction conditions for polysaccharides differed according to the different parts being extracted. Specifically, the optimal settings for extracting leaf polysaccharides comprised an extraction temperature at 70°C, a liquid-to-solid ratio of 40 mL/g, an ultrasonic time of 50 min, and an ultrasonic power setting of 249 W. Similarly, for pod polysaccharides, the optimal conditions were 70°C, 28 mL/g, 40 min and 201 W, respectively. Under the circumstances, the polysaccharide yield from leaf, and pod were 1.07 ± 0.20%, and 8.32 ± 0.27%, respectively, showing increments of up to 0.41 and 2.33% when compared to the traditional water extraction and alcohol precipitation method. Additionally, ultrasonic-assisted extraction technique decreased both the extraction duration and processing temperature, suggesting its efficacy in obtaining leaf and pod polysaccharides. The significantly lower yield of leaf polysaccharides compared to pod polysaccharides ($p < 0.05$) may result from advanced leaf lignification, which converts soluble polysaccharides into insoluble lignocellulose complexes, thereby reducing extractability. These findings align with report of Bai et al. (2022) on different parts of ginseng polysaccharide.

3.3 Chemical composition and purity analysis

Table 3 presented the total sugar, protein, uronic acid, polyphenol and flavonoid contents of crude polysaccharides extracted from leaf and pod of *A. julibrissin* before and after purification. As anticipated, significant differences in chemical composition were observed among the polysaccharides from various parts. The total sugar content of pod crude-AJPP was greater than that of crude-AJLP, indicating that the pod of *A. julibisin* had a richer polysaccharide content than the leaf. Similar results have also been reported by Shi et al. (2024), which may be due to the higher content of water-soluble impurities and pigments in the leaf of *A. julibrissin*. Besides, the protein content of crude-AJLP was higher than that of crude-AJPP, and it contained small amounts of polyphenol and flavonoid. These common impurities can affect the identification of polysaccharide

10.3389/fsufs.2025.1590775

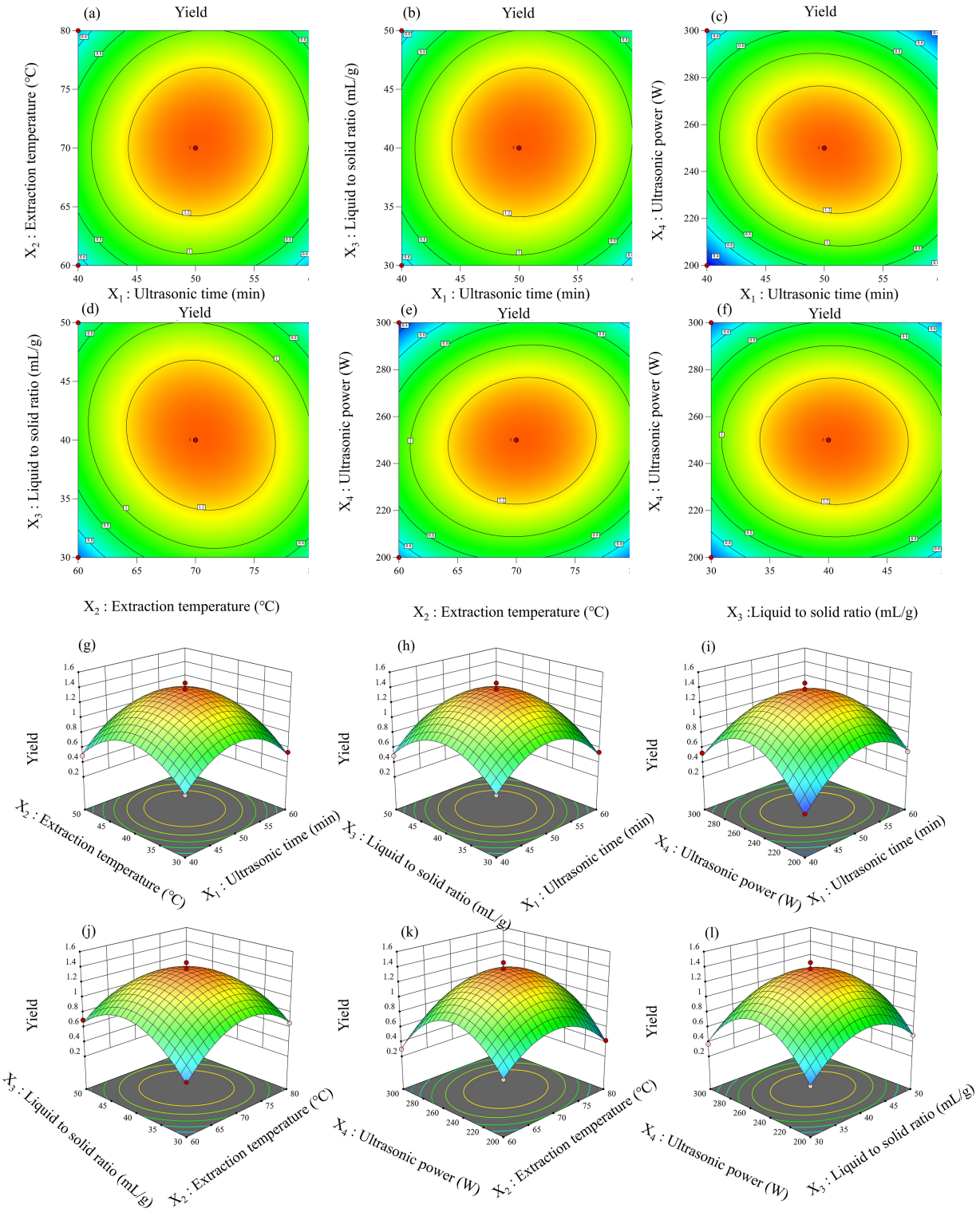

FIGURE 2
Response surfaces plots **(a–f)** and contour plots **(g–l)** of the interactive effects on the leaf polysaccharides yield.

structures and the study of their biological activities, so the Sevag method, DEAE-52 cellulose and dialysis were used for purification and separation. After purification, the presence of these impurities was not detected and the uronic acid content was increased. And they contained over 90% total sugar content and were suitable for subsequent experimental determinations.

3.4 FTIR analysis

This FTIR spectra absorption regions can facilitate the identification of polysaccharide functional groups (Zheng et al., 2024; Tang et al., 2024). The FT-IR spectra of AJLP and AJPP was presented in Figure 4. The approximate peaks at 3400 cm^{-1} and 2,900 cm^{-1}

10.3389/fsufs.2025.1590775

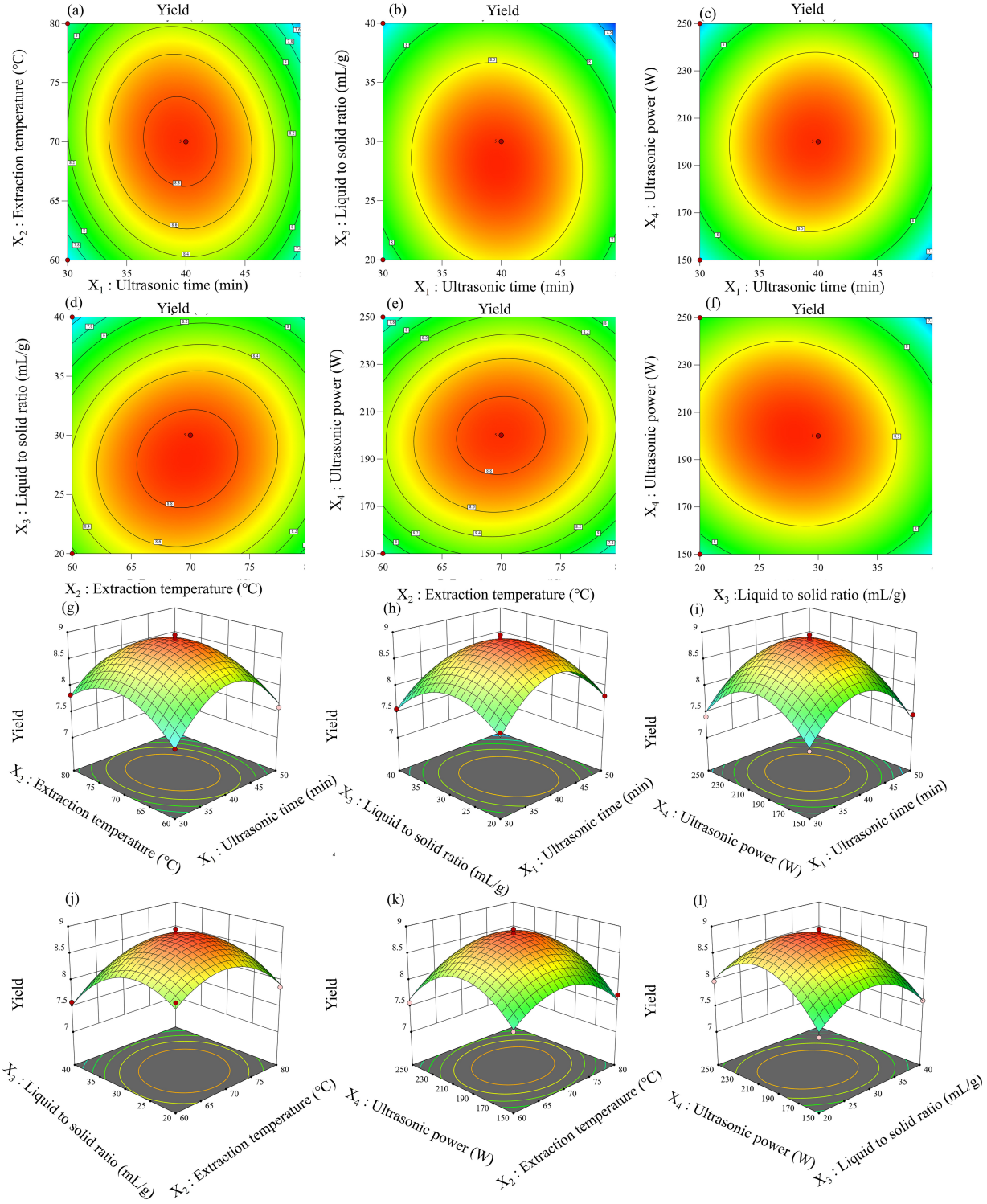

FIGURE 3
Response surfaces plots **(a–f)** and contour plots **(g–l)** of the interactive effects on the pod polysaccharides yield.

indicated O-H and C-H stretching vibrations, respectively. The spectral range from 1750 cm^{-1} to 1,600 cm^{-1} showed peaks indicative of C=O vibrations, hinting at the inclusion of uronic acid in the polysaccharide structure (He et al., 2016). Peaks observed between 1,500 and 1,200 cm^{-1} suggested C-H bond deformation vibrations. Additionally, multiple peaks in the 1,200 to 1,000 cm^{-1} range for AJLP and AJPP implied the presence of glycosidic linkages and pyran rings within the polysaccharide structure. Furthermore, the peaks observed within the 900 to 700 cm^{-1} range could potentially be associated with β-glycosidic bonds and α-glycosides (Zhang et al., 2018; Zhang et al.,

10.3389/fsufs.2025.1590775

TABLE 3 Comparison of the properties of AJLP and AJPP.

	AJLP	AJPP
Before purification		
Total sugar content (%)	7.69 ± 0.62	10.32 ± 0.62
Protein content (%)	6.71 ± 0.67	4.37 ± 0.59
Uronic acid content (%)	3.47 ± 0.74	2.87 ± 0.79
Polyphenol content (%)	3.14 ± 0.74	2.52 ± 0.64
Flavonoid content (%)	1.05 ± 0.69	1.26 ± 0.58
After purification		
Total sugar content (%)	91.67 ± 0.60	92.74 ± 0.72
Protein content (%)	–	–
Uronic acid content (%)	8.45 ± 0.80	7.38 ± 0.61
Polyphenol content (%)	–	–
Flavonoid content (%)	–	–

"–" was not detected.

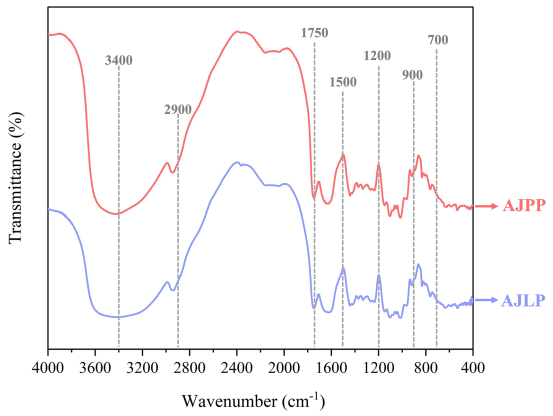

FIGURE 4
Fourier transform infrared spectroscopy (FT-IR) spectra of *Albizia julibrissin* leaf (AJLP) and *A. julibrissin* pod (AJPP).

2020). There was no significant difference in the infrared spectra among the AJLP and AJPP, which also was consistent with the previous report related to the *Angelica sinensis* (Oliv.) Diels polysaccharides (Zou et al., 2022), *Hibiscus manihot* L. polysaccharides (Shi et al., 2024) and different parts of ginseng polysaccharides (Bai et al., 2022).

3.5 Molecular weight distribution determination

The Mw can reflect the molecular chain information, exhibiting a profound correlation with the biological functionality of polysaccharides (Liang et al., 2023; Chen et al., 2024). In Figure 5 and Table 4, all of AJLP and AJPP showed two peaks, suggesting that they were composed of two polymers with distinct Mw. The broad peaks observed for AJLP and AJPP were due to the overlap of different polymer types. The Mw of the first fragment (peak 1) of AJLP (2.323×10^5 Da) is greater than that of the corresponding fragment of AJPP (8.051×10^4 Da). Similarly, the Mw of the second fragment (peak 2) also followed the same descending order. The findings indicated notable variations in the molecular weights of AJLP and AJPP, likely due to their origin from distinct parts and functions. High molecular weight polysaccharides may better facilitate the formation of membrane structures, participating in leaf support and water retention. Low molecular weight polysaccharides have higher water solubility, facilitating rapid metabolism and energy release during pod germination. Additionally, the polydispersity index, denoted as Mw/Mn, enables assessment of the uniformity in molecular weight distribution through the polydispersity coefficient. Table 4 revealed that the polysaccharide samples exhibited a polydispersity index between 1.0 and 1.1, suggesting a high level of homogeneity among the polysaccharides.

3.6 Monosaccharide composition analysis

Variations in monosaccharide compositions and their proportions significantly impact the structure and properties of polysaccharides (Zhang S. et al., 2023; Kong et al., 2023). The results of the experiment were depicted in Figure 6 and summarized in Table 5. It was noteworthy that the monosaccharide species composing AJLP and AJPP were the same, consisting of mannose, rhamnose, glucuronic acid, galacturonic acid, glucose, galactose, xylose and arabinose, but the proportions were obviously different. And the content of glucose, rhamnose, and galactose was relatively high, but the contents of glucuronic acid and xylose were the lowest. These differences in polysaccharide constituents could stem from distinct parts. Although the types of monosaccharide components remain unchanged, shifts in their content may affect the physicochemical characteristics and structure of these polysaccharides, potentially influencing their biological activities thereafter.

3.7 SEM analysis

Figure 7 illustrated the surface morphology of AJLP and AJPP captured by SEM at various magnifications: 200×, 500×, 1,000 × and 2000×. AJLP and AJPP displayed a disordered accumulation of flaky structures and rough surfaces, featuring prominent folds along the edges. In contrast, the microstructure of AJLP and AJPP was different, and the size of their flaky structure increasing sequentially from AJLP and AJPP. The differences in surface morphology might ascribe to the different degrees of branching in the two polysaccharides fractions (Zhu et al., 2021). A flatter surface could be observed under high magnification, the strong intermolecular interaction might be beneficial to exerting its bioactivity (Qu et al., 2019). Reports indicated that the dense structure is beneficial for polysaccharides to resist oral and gastrointestinal digestion, enabling them to reach the large intestine where they can be utilized by gut microbiota (Wang et al., 2025). These studies have found that polysaccharides extracted from the leaf and pod of *A. julibrissin* agro-byproducts have the potential to be developed into functional foods, health products, and medicines.

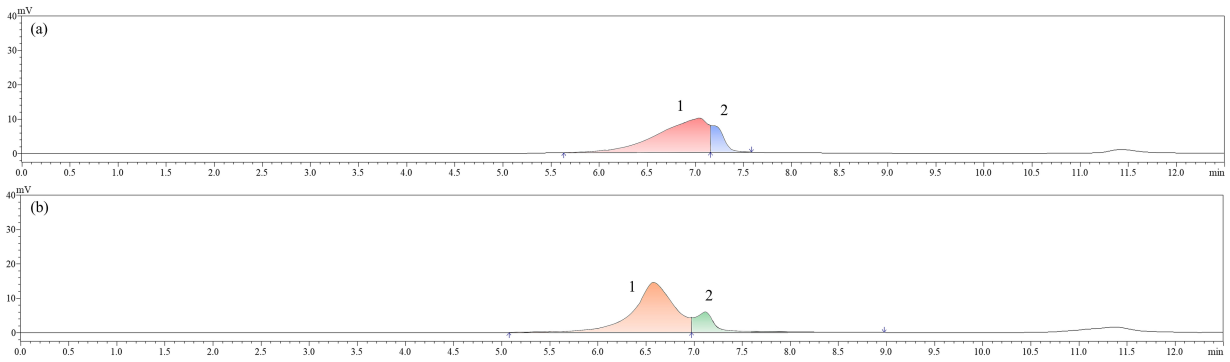

FIGURE 5
Molecular weight distribution by high performence gel permeation chromatography (HPGPC): *A. julibrissin* leaf (AJLP; **a**) and *A. julibrissin* pod (AJPP; **b**).

TABLE 4 Molecular weight distribution of AJLP and AJPP.

Name	Peaks	Peak area percentage (%)	Molecular weight (Da)	M_W/M_n
AJLP	1	83.85%	2.323×10^5	1.06
	2	16.14%	1.268×10^5	1.00
AJPP	1	82.51%	8.051×10^4	1.08
	2	17.48%	6.255×10^4	1.05

3.8 TGA analysis

TGA serves as a thermal analysis method, enabling the evaluation of crucial properties of polysaccharides, including their thermal stability and decomposition temperature (Dou et al., 2023; Lin et al., 2024). According to Figure 8, the thermal degradation of AJPP proceeded in two stages, whereas AJLP underwent degradation in four stages. During the initial stage, a minor weight reduction was observed at approximately 90°C, which may be due to the evaporation of water, both free and bound (Li et al., 2019). Variations were observed in the quantity of bound water, ranging between 5.10 and 9.06%. Notably, AJLP exhibited the highest weight loss (9.06%) at this stage, suggesting superior water retention capabilities. The second stage witnessed the greatest weight loss, primarily due to the depolymerization of polysaccharide chains and the decarboxylation of acid groups (Abubakar et al., 2024). During the third and fourth stages, the weight change of AJLP tended to stabilize, mainly because of the cleavage of sugar rings and the gradual development of a carbonized structure in the polysaccharide sample (Li et al., 2024; Xiao et al., 2019). The order of final weights is AJLP (39.96%) followed by AJPP (31.53%), indicating a variation in thermal stability, with AJLP exhibiting the highest and AJPP the lowest. Collectively, all polysaccharide fractions demonstrated commendable thermal stability and are applicable to high-temperature food processing. This disparity could potentially stem from variations in Mw, advanced structures and different parts. This finding has the potential to broaden the utilization of agro-byproducts (AJLP and AJPP) within the food industry.

3.9 Anticomplementary activity

The hemolytic assay reveals the drug's ability to inhibit complement activation, evidenced by its suppressive effect on red blood cell lysis induced by complement system activation. An investigation was conducted to evaluate the impact of AJLP and AJPP on the activation of the complement system via both the classical (CP) and alternative (AP) pathways, with heparin (CH_{50}: 0.143 ± 0.028 mg/mL; AP_{50}: 0.148 ± 0.037 mg/mL) serving as a positive control comparator. A pool of normal human serum served as the complement source for both the CP and AP. All results were presented in Table 6.

In an assay measuring anticomplementary activity through the CP, a 1:80 dilution of NHSP induced a 97.83 ± 0.76% hemolysis in antibody-sensitized sheep erythrocytes (EAs). The concentrations necessary to achieve 50% inhibition of hemolysis in EAs (CH_{50}) were found to be 0.122 ± 0.004 mg/mL for AJPP. In an assay measuring anticomplementary activity via the AP, a 1:8 dilution of NHSP induced a lysis of 96.90 ± 0.83% in rabbit erythrocytes (ERs). The AP_{50} values, which represent the concentrations causing 50% inhibition of hemolysis in ERs, were determined to be 0.070 ± 0.003 mg/mL for AJLP. AJLP demonstrated no inhibitory activity against complement activation via the CP, while AJPP showed no such activity against activation through the AP. In CP, the polysaccharides obtained from the leaf were comparable to the positive drug heparin in terms of complement inhibitory capacity. Notably, the polysaccharides derived from the pod exhibited significantly higher anticomplementary activity than heparin in AP. The results of this experiment were encouraging, the often-neglected agro-byproducts (leaf and pod) possessed inhibitory abilities comparable to or even superior to those of heparin as a positive control drug. It was interesting to note that the complement inhibition by the leaf and pod was via a single pathway, which will enable them to have a more specific therapeutic effect on related diseases caused by a certain pathway. Even in the field of functional foods and health products, AJLP and AJPP have great potential for development. This offers a fresh perspective on the holistic development and utilization of Traditional Chinese Medicine, ensuring efficient use of active ingredients and generating substantial economic benefits.

10.3389/fsufs.2025.1590775

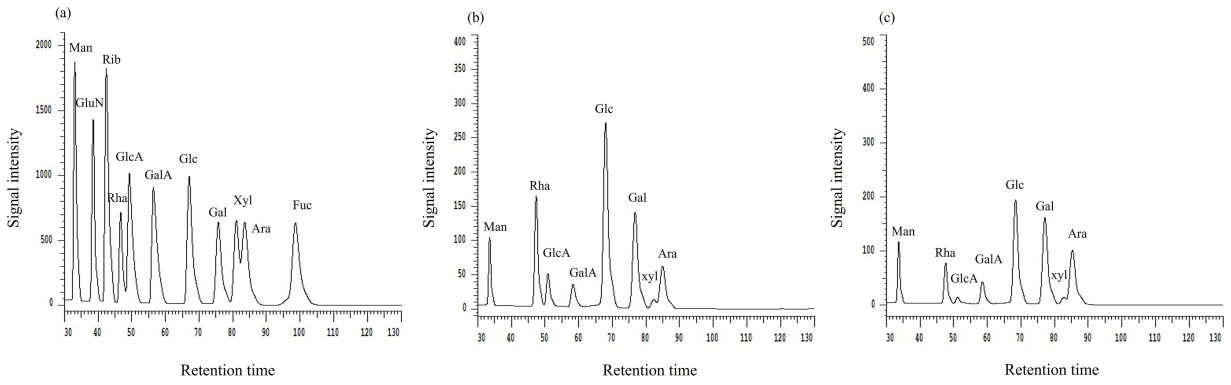

FIGURE 6
High performance liquid chromatography (HPLC) chromatograms of monosaccharide standard samples **(a)**, **A**. *julibrissin* leaf (AJLP; **b**) and *A. julibrissin* pod (AJPP; **c**). "Man" denotes mannose, "Rha" denotes rhamnose, "GlcA" denotes glucuronic acid, "GalA" denotes galacturonic acid, "Glc" denotes glucose, "Gal" denotes galactose, "Xyl" denotes xylose, "Ara" denotes arabinose.

TABLE 5 Monosaccharides composition of AJLP and AJPP.

Monosaccharide composition (molar ratio)	AJLP	AJPP
Mannose	6.00	10.54
Rhamnose	18.95	12.85
Glucuronic acid	3.85	2.38
Galacturonic acid	3.90	7.00
Glucose	39.85	47.46
Galactose	16.80	29.69
Xylose	1.00	1.00
Arabinose	5.55	16.62

4 Conclusion

This study represents the first systematic investigation of polysaccharides extracted from *Albizia julibrissin* Durazz. leaf and pod (agricultural by-products), utilizing optimized ultrasound-assisted extraction. And comprehensively characterized two polysaccharides (AJLP and AJPP), comparing their physicochemical properties, functional features, and anticomplementary activity, elucidating their potential as natural complement inhibitor. The results demonstrated that AJLP and AJPP contained both β-glycosidic and α-glycosidic bonds, with significant molecular weight differences among polysaccharide fractions (from 2.323×10^5 Da to 6.255×10^4 Da). Notably, AJLP and AJPP exhibited identical monosaccharide compositions (mannose, rhamnose, glucuronic acid, galacturonic acid, glucose, galactose, xylose, and arabinose) but distinct molar ratios. In addition, AJLP and AJPP exhibited good thermal stability. The hemolysis assay confirmed the potent anticomplementary activity of AJPP ($CH_{50} = 0.122 \pm 0.004$ mg/mL) and AJLP ($AP_{50} = 0.070 \pm 0.003$ mg/mL), suggesting therapeutic potential for overactivation of the complement system disorders and aiding in their classification and utilization. This study expanded the current data on the anticomplementary activity of polysaccharides sourced from traditional Chinese medicines and established a theoretical groundwork for the further comprehensive utilization of each medicinal part. Recycling agricultural by-products in this way will reduce environmental impact while establishing a theoretical foundation for advancing *A. julibrissin* polysaccharide-based product development.

Data availability statement

The original contributions presented in the study are included in the article/supplementary material, further inquiries can be directed to the corresponding authors.

Ethics statement

The animal study was approved by Ethical approval was also obtained from Yanbian University's Ethics Committee, with approval number YBU-2018-090401. The study was conducted in accordance with the local legislation and institutional requirements.

Author contributions

YD: Conceptualization, Data curation, Methodology, Writing – original draft, Writing – review & editing. YJ: Formal analysis, Investigation, Writing – review & editing. JG: Investigation, Methodology, Writing – review & editing. CS: Formal analysis, Methodology, Writing – review & editing. BS: Formal analysis, Methodology, Writing – review & editing. YX: Formal analysis, Methodology, Writing – review & editing. LJ: Methodology, Writing – review & editing. MJ: Methodology, Formal analysis, Validation, Writing – review & editing. JS: Conceptualization, Project administration, Supervision, Writing – review & editing. WZ: Project administration, Resources, Supervision, Writing – review & editing. ZH: Methodology, Project administration, Writing – review & editing. GL: Conceptualization, Project administration, Resources, Writing – review & editing.

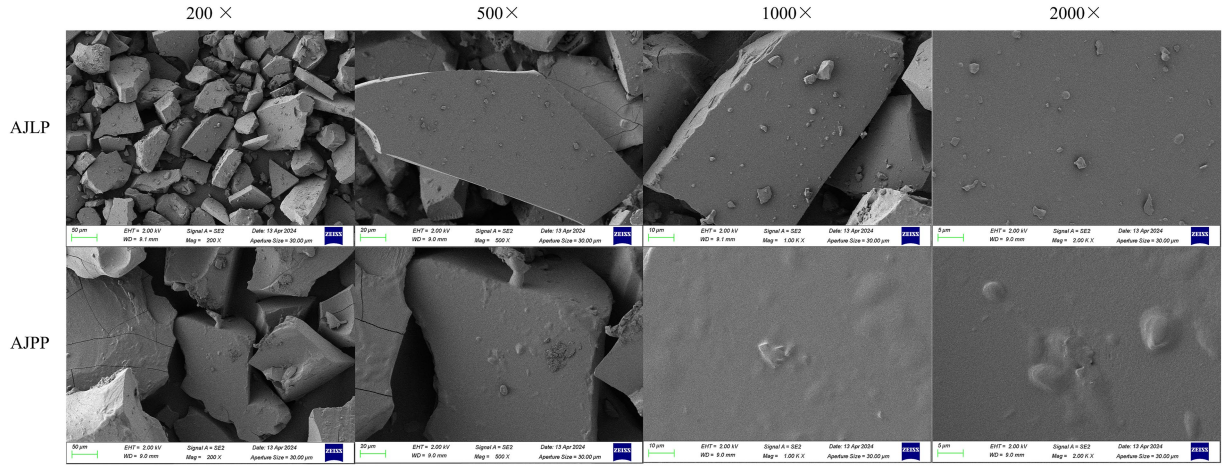

FIGURE 7
Scanning electron micrographs of *A. julibrissin* leaf (AJLP) and *A. julibrissin* pod (AJPP).

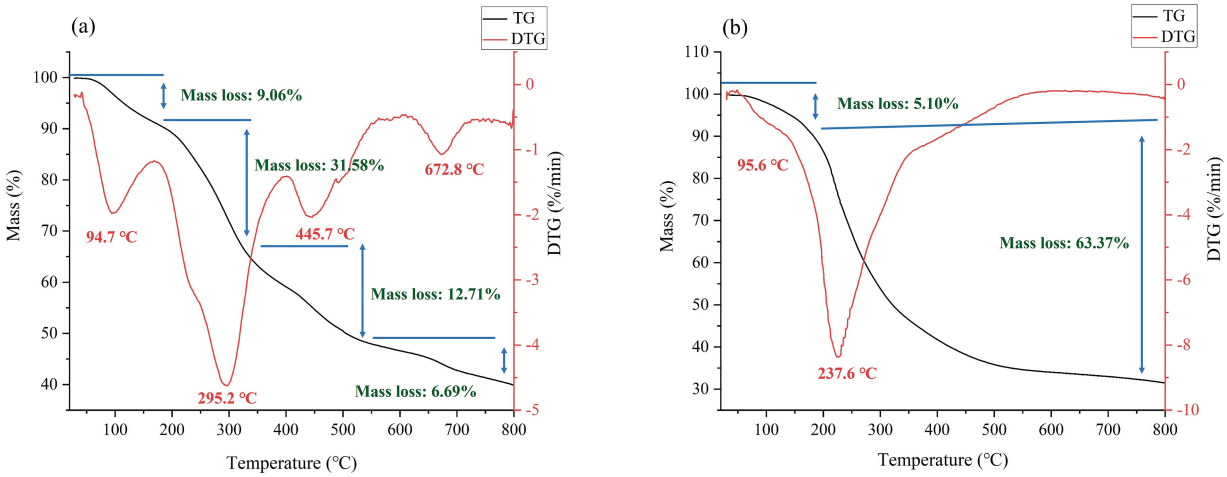

FIGURE 8
TG and DTG curves of *A. julibrissin* leaf (AJLP; **a**) and *A. julibrissin* pod (AJPP; **b**).

TABLE 6 50% hemolytic inhibition concentrations of AJLP and AJPP.

	AJLP	AJPP	Heparin
CH_{50} (mg/mL)	NE	0.122 ± 0.004[a]	0.143 ± 0.028[a]
AP_{50} (mg/mL)	0.070 ± 0.003[b]	NE	0.148 ± 0.037[a]

Different letters indicate significant difference ($p < 0.05$). "NE" denotes that this sample has no inhibitory effect at the maximal concentration that was tested. CH_{50}: 50% inhibition of hemolysis in EAs. CP_{50}: 50% inhibition of hemolysis in ERs.

Funding

The author(s) declare that financial support was received for the research and/or publication of this article. This research was supported by the grant from the National Natural Science Foundation of China (grant nos. 82360683, 82360805, and 82260834), Jilin Provincial Science and Technology Department (grant no. 20230508170RC), Jilin Provincial Education Department (grant no. JJKH20220557KJ), Health Commission of Jilin Provincial (grant no. 2019Q022) and Yanbian University Doctoral Initiation Fund Project (grant no. ydbq202428).

Conflict of interest

The authors declare that the research was conducted in the absence of any commercial or financial relationships that could be construed as a potential conflict of interest.

Generative AI statement

The author(s) declare that no Gen AI was used in the creation of this manuscript.

Publisher's note

References

Abubakar, A., Ahmad, B., Ahmad, N., Liu, L., Liu, B., Qu, Y., et al. (2024). Physicochemical evaluation, structural characterization, in vitro and in vivo bioactivities of water-soluble polysaccharides from Luobuma (*Apocynum* L.) tea. *Food Chem.* 460:140453. doi: 10.1016/j.foodchem.2024.140453

Andrew, C. G., Norbert, P. L., Nita, S., William, D. M., Arthur, J. W., Kelly, M. L., et al. (2024). Reconstitution of the alternative pathway of the complement system enables rapid delineation of the mechanism of action of novel inhibitors. *J. Biol. Chem.* 300:107467. doi: 10.1016/j.jbc.2024.107467

Bai, C., Chen, R., Tan, C., Bai, H., Tian, B., Lu, J., et al. (2022). Effects of multi-frequency ultrasonic on the physicochemical properties and bioactivities of polysaccharides from different parts of ginseng. *Int. J. Biol. Macromol.* 206, 896–910. doi: 10.1016/j.ijbiomac.2022.03.098

Chen, Z., Wang, C., Su, J., Liang, G., Tan, S., Bi, Y., et al. (2024). Extraction of *Pithecellobium clypearia Benth* polysaccharides by dual-frequency ultrasound-assisted extraction: structural characterization, antioxidant, hypoglycemic and anti-hyperlipidemic activities. *Ultrason. Sonochem.* 107:106918. doi: 10.1016/j.ultsonch.2024.106918

Dou, Z., Zhang, Y., Tang, W., Deng, Q., Hu, B., Chen, X., et al. (2023). Ultrasonic effects on the degradation kinetics, structural characteristics and protective effects on hepatocyte lipotoxicity induced by palmitic acid of *Pueraria Lobata* polysaccharides. *Ultrason. Sonochem.* 101:106652. doi: 10.1016/j.ultsonch.2023.106652

Duan, Y. Q., Hu, Z. Y., Jin, L., Zong, T. Q., Zhang, X. H., Liu, Y. N., et al. (2024). Efficient degradation and enhanced anticomplementary activity of *Belamcanda chinensis* (L.) DC. Polysaccharides via trifluoroacetic acid treatment with different degrees. *Int. J. Biol. Macromol.* 276:134117. doi: 10.1016/j.ijbiomac.2024.134117

Han, L., Pan, G., Wang, Y., Song, X., Gao, X., Ma, B., et al. (2011). Rapid profiling and identification of triterpenoid saponins in crude extracts from *Albizia julibrissin* Durazz. By ultra high-performance liquid chromatography coupled with electrospray ionization quadrupole time-of-flight tandem mass spectrometry. *J. Pharmaceut. Biomed.* 55, 996–1009. doi: 10.1016/j.jpba.2011.04.002

Hao, Y. J., Zhang, K. X., Jin, M. Y., Piao, X. C., Lian, M. L., and Jiang, J. (2023). Improving fed-batch culture efficiency of Rhodiola sachalinensis cells and optimizing flash extraction process of polysaccharides from the cultured cells by BBD-RSM. *Ind. Crop. Prod.* 196:116513. doi: 10.1016/j.indcrop.2023.116513

He, T., Huang, Y., Yang, L., Liu, T., Gong, W., Wang, X., et al. (2016). Structural characterization and immunomodulating activity of polysaccharide from *Dendrobium officinale*. *Int. J. Biol. Macromol.* 83, 34–41. doi: 10.1016/j.ijbiomac.2015.11.038

He, Y., Wang, Q., Ye, Y., Liu, Z., and Sun, H. (2020). Anti-tumor target identification and molecular mechanism study of total saponins from *Albizia julibrissin*. *J. Ethnopharmacol.* 257:112677. doi: 10.1016/j.jep.2020.112677

Huang, B., Wu, Y., Li, C., Tang, Q., and Zhang, Y. (2023). Molecular basis and mechanism of action of *Albizia julibrissin* in depression treatment and clinical application of its formulae. *Chin. Herb. Med.* 15, 201–213. doi: 10.1016/j.chmed.2022.10.004

Jacqui, N., Byrne, R., Daskoulidou, N., Watkins, L. M., Carpanini, S. M., Zelek, W. M., et al. (2024). The complement system in neurodegenerative diseases. *Clin. Sci.* 138, 387–412. doi: 10.1042/CS20230513

Jean, F., Natalia, M., Renata, R., Marcello, I., Lauro, M., Fernanda, F., et al. (2025). The use of Pleurotus ostreatus by-products for the preparation of a gel-like polysaccharide with bioactive properties. *Int. J. Biol. Macromol.* 301:140236. doi: 10.1016/j.ijbiomac.2025.140236

Ji, H., Liu, C., Dai, K., Yu, J., Liu, A., and Chen, Y. (2021). The extraction, structure, and immunomodulation activities in vivo of polysaccharides from *Salvia miltiorrhiza*. *Ind. Crop. Prod.* 173:114085. doi: 10.1016/j.indcrop.2021.114085

Kanlayavattanakul, M., Pawakongbun, T., and Lourith, N. (2019). Dendrobium orchid polysaccharide extract: preparation, characterization and in vivo skin hydrating efficacy. *Chin. Herb. Med.* 11, 400–405. doi: 10.1016/j.chmed.2019.03.012

Kong, T., Liu, S., Feng, Y., Fan, Y., Yyu, J., Zhang, H., et al. (2023). Slit dual-frequency ultrasound-assisted pulping of *Lycium barbarum* fresh fruit to improve the dissolution of polysaccharides and in situ real-time monitoring. *Ultrason. Sonochem.* 98:106569. doi: 10.1016/j.ultsonch.2023.106509

Lau, C. S., Carrier, D. J., Beitle, R. R., Bransby, D. I., Howard, L. R., Lay, J., et al. (2007). Identication and quantication of glycoside Xavonoids in the energy crop *Albizia julibrissin*. *Bioresour. Technol.* 98, 429–435. doi: 10.1016/j.biortech.2005.12.011

Li, Q., Li, J., Li, H., Xu, R., Yuan, Y., and Cao, J. (2019). Physicochemical properties and functional bioactivities of different bonding state polysaccharides extracted from tomato fruit. *Carbohydr. Polym.* 219, 181–190. doi: 10.1016/j.carbpol.2019.05.020

Li, C., Zhang, Q., Yin, C., Gao, H., Fan, X., Shi, D., et al. (2024). γ-Irradiation effects on the physicochemical properties and biological activities of *Schizophyllum commune* polysaccharides. *Radiat. Phys. Chem.* 221:111734. doi: 10.1016/j.radphyschem.2024.111734

Li, Y., Zhu, X., Zhai, X., Zhang, Y., Duan, Z., and Sun, J. (2018). Optimization of enzyme assisted extraction of polysaccharides from pomegranate peel by response surface methodology and their anti-oxidant potential. *Chin. Herb. Med.* 10, 416–423. doi: 10.1016/j.chmed.2018.08.007

Liang, L., Yue, Y., Zhong, L., Liang, Y., Shi, R., Luo, R., et al. (2023). Anti-aging activities of *Rehmannia glutinosa* Libosch. Crude polysaccharide in *Caenorhabditis elegans* based on gut microbiota and metabonomic analysis. *Int. J. Biol. Macromol.* 253:127647. doi: 10.1016/j.ijbiomac.2023.127647

Lin, P., Wang, Q., Wang, Q., Chen, J., He, L., Qin, Z., et al. (2024). Evaluation of the anti-atherosclerotic effect for *Allium macrostemon* Bge. Polysaccharides and structural characterization of its a newly active fructan. *Carbohydr. Polym.* 340:122289. doi: 10.1016/j.carbpol.2024.122289

Liu, S., Shi, X., Xiang, W., Jin, Z., Jia, Y., Zhang, Y., et al. (2023). Bioactivities and physicochemical properties of crude polysaccharides from mulberry twigs, agricultural by-products. *Ind. Crop. Prod.* 193:116191. doi: 10.1016/j.indcrop.2022.116191

Liu, J., Zhou, J., Zhang, Q., Zhu, M., Hua, M., and Xu, Y. (2019). Monosaccharide analysis and fingerprinting identification of polysaccharides from *Poria cocos* and *Polyporus umbellatus* by HPLC combined with chemometrics methods. *Chin. Herb. Med.* 11, 406–411. doi: 10.1016/j.chmed.2019.05.008

Lu, P., Zhang, C., Zheng, J., Li, C., Zhang, Q., and Huang, B. (2023). Research progress on chemical components and pharmacological effects of the flowers of *Albizia julibrissin* Durazz. *J. Ethnopharmacol.* 303:116002. doi: 10.1016/j.jep.2022.116002

Nehid, I. (2011). Characteristics, chemical composition and utilisation of *Albizia julibrissin* seed oil. *Ind. Corp. Pord.* 33, 30–34. doi: 10.1016/j.indcrop.2010.08.004

Niu, J., Xu, G., Jiang, S., Li, H., and Yuan, G. (2017). In vitro antioxidant activities and anti-diabetic effect of a polysaccharide from *Schisandra sphenanthera* in rats with type 2 diabetes. *Int. J. Biol. Macromol.* 94, 154–160. doi: 10.1016/j.ijbiomac.2016.10.015

Qu, H., Gao, X., Zhao, H., Wang, Z., and Yi, J. (2019). Structural characterization and in vitro hepatoprotective activity of polysaccharide from pine nut (*Pinus koraiensis Sieb. Et Zucc.*). *Carbohydr. Polym.* 223:115056. doi: 10.1016/j.carbpol.2019.115056

Ruth, F., and Howard, M. (2022). The role of anticomplement therapy in lupus nephritis. *Transl. Res.* 245, 1–17. doi: 10.1016/j.trsl.2022.02.001

Shi, H., Li, J., Yu, J., Li, H., Huang, G., and Zhang, T. (2024). Extraction, purification and antioxidant activity of polysaccharides from different parts of *Hibiscus manihot* L. *J. Mol. Struct.* 1295:136598. doi: 10.1016/j.molstruc.2023.136598

Tang, Z., Huang, G., and Huang, H. (2024). Ultrasonic-assisted extraction, analysis and properties of purple mangosteen scarfskin polysaccharide and its acetylated derivative. *Ultrason. Sonochem.* 109:107010. doi: 10.1016/j.ultsonch.2024.107010

Wang, X., Jiao, Y., Zhu, H., Lu, Y., and Chen, D. (2023). Exploring the anticomplement components from Fagopyrum dibotrys for the treatment of H1N1-induced acute lung injury by UPLC-triple-TOF-MS/MS. *J. Pharmaceut. Biomed.* 223:115158. doi: 10.1016/j.jpba.2022.115158

Wang, W., Liu, X., Wang, L., Song, G., Jiang, W., Mu, L., et al. (2023). *Ficus carica* polysaccharide extraction via ultrasound-assisted technique: structure characterization, antioxidant, hypoglycemic and immunomodulatory activities. *Ultrason. Sonochem.* 101:106680. doi: 10.1016/j.ultsonch.2023.106680

Wang, J., Sun, J., Jin, L., Wang, M., Huang, Y., Jin, M., et al. (2022). One novel naphthalene derivative and other constituents with anti-complementary activities from the aerial parts of *Dracocephalum moldavica*. *J. Asian Nat. Prod. Res.* 24, 1177–1184. doi: 10.1080/10286020.2021.2024518

Wang, L., Zhang, Z., Zeng, Z., Lin, Y., Xiong, B., Zheng, B., et al. (2025). Structural characterization of polysaccharide from an edible fungus *Dictyophora indusiata* and the remodel function of gut microbiota in inflammatory mice. *Carbohydr. Polym.* 351:123141. doi: 10.1016/j.carbpol.2024.123141

Xiao, Y., Liu, S., Shen, M., Jiang, L., Ren, Y., Luo, Y., et al. (2019). Physicochemical, rheological and thermal properties of *Mesona chinensis* polysaccharides obtained by sodium carbonate assisted and cellulase assisted extraction. *Int. J. Biol. Macromol.* 126, 30–36. doi: 10.1016/j.ijbiomac.2018.12.211

Xiu, W., Wang, X., Na, Z., Yu, S., Wang, J., Yang, M., et al. (2023). Ultrasound-assisted hydrogen peroxide-ascorbic acid method to degrade sweet corncob polysaccharides can help treat type 2 diabetes via multiple pathways in vivo. *Ultrason. Sonochem.* 101:106683. doi: 10.1016/j.ultsonch.2023.106683

Xu, W., Zhou, W., Sun, J., Chen, W., Wu, X., Guan, T., et al. (2024). Isolation, structural characterization, and hypoglycemic activity of polysaccharides from the stems of *Panax ginseng* C. A. Meyer. *Front. Sustain. Food Syst.* 8:1500278. doi: 10.3389/fsufs.2024.1500278

Yuan, G., Wang, Y., Niu, H., Ma, Y., and Song, J. (2024). Isolation, purification, and physicochemical characterization of *Polygonatum* polysaccharide and its protective effect against CCl_4-induced liver injury via Nrf2 and NF-κB signaling pathways. *Int. J. Biol. Macromol.* 261:129863. doi: 10.1016/j.ijbiomac.2024.129863

Zhang, W., Duan, W., Huang, G., and Huang, H. (2023). Ultrasonic-assisted extraction, analysis and properties of mung bean peel polysaccharide. *Ultrason. Sonochem.* 98:106487. doi: 10.1016/j.ultsonch.2023.106487

Zhang, Z., Guo, L., Yan, A., Feng, L., and Wan, Y. (2020). Fractionation, structure and conformation characterization of polysaccharides from *Anoectochilus roxburghii*. *Carbohydr. Polym.* 231:115688. doi: 10.1016/j.carbpol.2019.115688

Zhang, Y., Liu, Y., Cai, Y., Tian, Y., Xu, L., Zhang, A., et al. (2023). Ultrasonic-assisted extraction brings high-yield polysaccharides from Kangxian flowers with cosmetic potential. *Ultrason. Sonochem.* 100:106626. doi: 10.1016/j.ultsonch.2023.106626

Zhang, Y., Sun, M., He, Y., Gao, G., Wang, Y., Yang, B., et al. (2024). Extraction, optimization, and biological activities of a low molecular weight polysaccharide from *Platycodon grandifloras. Int. J. Biol. Macromol.* 271:132617. doi: 10.1016/j.ijbiomac.2024.132617

Zhang, S., Waterhouse, G., Xu, F., Ge, Z., Du, Y., Lian, Y., et al. (2023). Sun-Waterhouse, recent advances in utilization of pectins in biomedical applications: a review focusing on molecular structure-directing health-promoting properties. *Crit. Rev. Food Sci.* 63, 3386–3419. doi: 10.1080/10408398.2021.1988897

Zhang, Q., Xu, Y., Lv, J., Cheng, M., Wu, Y., Cao, K., et al. (2018). Structure characterization of two functional polysaccharides from *Polygonum multiflorum* and its immunomodulatory. *Int. J. Biol. Macromol.* 113, 195–204. doi: 10.1016/j.ijbiomac.2018.02.064

Zheng, C., Li, T., Tang, Y., Lu, T., Wu, M., Sun, J., et al. (2024). Structural and functional investigation on stem and peel polysaccharides from different varieties of pitaya. *Int. J. Biol. Macromol.* 259:129172. doi: 10.1016/j.ijbiomac.2023.129172

Zheng, Q., Ren, D., Yang, N., and Yang, X. (2016). Optimization for ultrasound-assisted extraction of polysaccharides with chemical composition and antioxidant activity from the *Artemisia sphaerocephala* Krasch seeds. *Int. J. Biol. Macromol.* 91, 856–866. doi: 10.1016/j.ijbiomac.2016.06.042

Zhu, M., Huang, R., Wen, P., Song, Y., He, B., Tan, J., et al. (2021). Structural characterization and immunological activity of pectin polysaccharide from kiwano (*Cucumis metuliferus*) peels. *Carbohydr. Polym.* 254:117371. doi: 10.1016/j.carbpol.2020.117371

Zou, Y., Li, C., Fu, Y., Jiang, Q., Peng, X., Li, L., et al. (2022). The comparison of preliminary structure and intestinal anti-inflammatory and anti-oxidative activities of polysaccharides from different root parts of *Angelica sinensis* (Oliv.) Diels. *J. Ethnopharmacol.* 295:115446. doi: 10.1016/j.jep.2022.115446